CORE
Metadata, citation and similar papers at core.ac.uk
Provided by University of Bath Research Portal

Citation for published version:
Bibi, S, Price, GJ, Yasin, T & Nawaz, M 2016, 'Eco-friendly synthesis and catalytic application of chitosan/gold/carbon nanotube nanocomposite films', RSC Advances, vol. 6, no. 65, pp. 60180-60186. https://doi.org/10.1039/c6ra11618c

DOI:
10.1039/c6ra11618c

Publication date:
2016

Document Version
Peer reviewed version

Link to publication

University of Bath

General rights
Copyright and moral rights for the publications made accessible in the public portal are retained by the authors and/or other copyright owners and it is a condition of accessing publications that users recognise and abide by the legal requirements associated with these rights.

Take down policy
If you believe that this document breaches copyright please contact us providing details, and we will remove access to the work immediately and investigate your claim.

Download date: 13. May. 2019

Eco-friendly synthesis and catalytic application of Chitosan/Gold/Carbon Nanotube nanocomposite films

Saira Bibi[a,b,*], Gareth Price[c], Tariq Yasin[b], Mohsan Nawaz[a]

a. *Department of Chemistry, Hazara University, Mansehra, Pakistan.*
b. *Pakistan Institute of Engineering and Applied Sciences, Islamabad, Pakistan*
c. *Department of Chemistry, University of Bath, Claverton Down, Bath, BA2 7AY, UK*

Novel eco-friendly chitosan nanocomposite membranes containing gold nanoparticles and carbon nanotubes (CNTs) have been synthesized. The catalytic activity of the nanocomposites was explored using a model reduction reaction of 4-nitrophenol to 4-aminophenol. Kinetic studies demonstrated that the presence of CNTs increased the rate of the reaction, mainly by reducing the induction time. TEM images confirmed the uniform distribution of gold and CNTs in the chitosan matrices. Scanning electron microscopy micrographs revealed that the inclusion of CNTs led to a more compact and less porous network structure which improved the mechanical properties of the films. Catalytically active membranes prepared from the nanocomposites could be reused at least ten times with no loss of mechanical integrity or catalytic effect, opening up the possibility of using this new, environmentally-friendly catalyst support in a continuous flow system.

Gold NPs on carbon nanotubes in a chitosan matrix form a reusable (> 10 times), highly active catalyst system

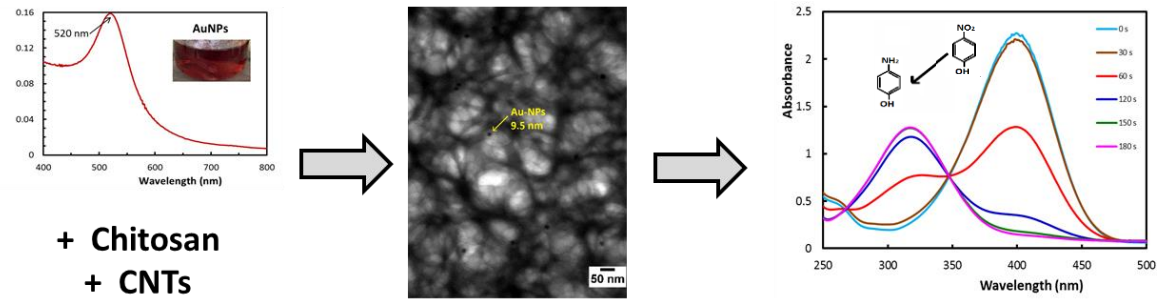

Introduction

Gold nanoparticles (Au-NPs) have shown remarkable potential for a wide range of applications due to their unusual optical, chemical, photo-electrochemical and catalytic properties.[1-4] However their high surface activity leads to a tendency to aggregate, reducing their activity as catalysts.[5] This can be overcome by dispersing the NPs within a suitable support.[6] For this purpose, both synthetic and natural polymers have been used.[7-9] For example, Kurodo *et al*. dispersed Au-NPs onto poly(methyl methacrylate) beads and reported excellent catalytic activity for the reduction of 4-nitrophenol.[10] The current quest for cleaner and more sustainable materials makes replacing petrochemical-based feedstocks with bio-based, natural polymers for support materials desirable.[11] Using a natural polymer as the support matrix into which to disperse catalytic NPs could not only be a more sustainable option but also reduce the environmental impact of their disposal after use. Many such polymers contain large numbers of hydrophilic groups which facilitate the dispersion and stabilization of NPs.[12, 13]

Chitosan is a natural, biodegradable polysaccharide comprising both glucosamine and acetyl-glucosamine units.[14] Its flexibility and membrane-forming ability as well as its insolubility in most solvents together with the large number of functional groups have been exploited in applications such as metal ion sorption, drug delivery and catalysis.[15] Chitosan is an excellent candidate as a sustainable support for catalysts[16, 17] as demonstrated by Guo *et al*.[18] who reported the aerobic oxidation of cyclohexane by chitosan/iron tetraphenylporphyrin. Chitosan membranes containing palladium were used by Zeng *et al*.[19] for the heterogeneous catalysis of cross-coupling reactions.

The mechanical frailty of chitosan can be reduced by blending with flexible polymers, by crosslinking or by adding nanofillers.[20, 21] Reinforcing chitosan with carbon nanotubes (CNTs) has been shown to enhance its thermo-mechanical properties.[22] Recently, Aztatzi-Pluma *et al*.[23] demonstrated the nature of the molecular interactions between functionalized CNTs and chitosan.

CNTs are inherently inert but easily agglomerate and entangle due to strong van der Waals interactions.[24] To overcome this, CNTs have been functionalized using a number of chemical methods and also by irradiation techniques.[25-27] The use of ionizing radiation for functionalizing CNTs is a potentially cleaner approach than using wet-chemical methods. It is very effective in creating functional groups on the surface of the CNTs. Adding irradiated CNTs to a chitosan matrix could potentially improve the thermo-mechanical performance as well as providing a large surface area to coordinate the catalyst.[28-32] Moreover, functionalized CNTs could enhance catalysis by coordinating substrate molecules through a range of non-covalent bonding interactions as well as by enhancing the accessibility of substrate molecules.[33]

Aromatic amines are key intermediates in many agricultural chemicals as well as in surfactants, polymers and dyeing agents. Conventionally, catalytic hydrogenation and other chemical reduction methods have been employed.[34, 35] The widely used iron-HCl

system requires large amounts of iron which makes the process costly and generates toxic waste and effluent (typically 1.2 kg of Fe-FeO sludge per kg of product).[36] Thus the overall process is environmentally hazardous and there is a growing need to replace it with cleaner, non-toxic, reusable and eco-friendly methods.[37]

This study introduces such an efficient, eco-friendly nanocatalyst system which potentially overcomes these environmental problems. Chemical free functionalization of CNTs was performed using gamma irradiation. Both Au-NPs and functionalized CNTs have been incorporated into a chitosan matrix and crosslinked using small amounts of vinyl triethoxy silane (VTES). Catalysis of the reduction of 4-nitrophenol to 4-aminophenol (4-AP) using sodium borohydride, a comparatively mild and cleaner reducing agent, has been investigated as a model reaction.

Experimental

Chemicals and materials

Gold chloride, 4-nitrophenol (4-NP), 4-aminophenol (4-AP), sodium borohydride ($NaBH_4$), chitosan (C3646, 75% deactylated), poly(vinyl alcohol) (PVA, Mw: 146,000-186,000), poly(vinyl pyrrolidone) (PVP, average Mw: 40,000), tetraethylorthosilicate, (TEOS), VTES, potassium persulfate (KPS), acetic acid, sodium hydroxide, hydrochloric acid and ethanol were obtained from Sigma-Aldrich (UK) and used without further purification. CNTs, diameter 9.5 nm, and average length 1.5 µm were purchased from Korea (NANOCYL). CNTs were treated with gamma radiation at Pakistan Radiation Services using ^{60}Co gamma irradiator (Model JS-7900, IR-148, ATCOP) in air at a dose rate of 1.02 kGy/h to give a total absorbed dose of 200 kGy.

Synthesis of Gold nanoparticles

Au-NPs were synthesized by a previously reported method.[38] A solution of gold chloride, $HAuCl_4$, (1.25×10^{-4} M, 300 cm^3) was boiled and 3 cm^3 of sodium citrate (0.05 M) solution added swiftly whilst stirring. On cooling, the pale purple solution changed to ruby-red indicating the formation of Au-NPs by the reduction by citrate of soluble Au (I) to insoluble Au (0). The presence of Au-NPs was confirmed by observing the peak around 520 nm in the UV-Vis absorbance spectrum.

Preparation of nanocomposites

Gold nanoparticles were dispersed in chitosan to give a nanocomposite – indicated here by Chi/Au - by modifying a previously published procedure.[39] Chitosan (1.8 g) was dissolved in 100 cm^3 of 2% (w/v) acetic acid and 50 cm^3 of Au-NPs from the above suspension was dispersed into the solution using an ultrasonic horn (Sonic Processor L500-20, Sonic Systems) for 10 min at an intensity of 12 W cm^{-2}. PVA and PVP (10 mg each) were separately dissolved in 10 cm^3 water. The solutions were mixed and VTES

(15.5 µL) and KPS (12.5 mg) added before heating to 70 °C for 1 h. The mixture was then added to the chitosan solution containing TEOS (15.5 µL, hydrolyzed) and sonicated for 1 h at 45°C under the same conditions as above. After 1 h sonication, the solution was poured into dishes and allowed to dry at room temperature. To prepare nanocomposites containing both AuNPs and CNTs – indicated by Chi/Au/CNTs - the same procedure was used except that 1.25 mg of CNTs was dispersed in the PVP solution using the ultrasound horn before mixing with the PVA solution.

Measurements and characterization

UV-visible spectra were recorded on an Agilent-8453 spectrophotometer using a quartz cell with path length 0.10 cm. For Transmission Electron Microscope (TEM) studies of Au-NPs, 1.0 µL of the aqueous suspension was placed on a carbon-coated Cu-grid (200 mesh) and the solvent allowed to evaporate at room temperature. After drying the samples were kept in a vacuum desiccator overnight. TEM measurements were carried out on a JEOL JEM 1200 EXII instrument operated at an accelerating voltage of 120.0 kV. To image the nanocomposites, a small amount was suspended in ethanol by sonication for 30 s and 1.0 µL was dropped onto a Cu-grid and allowed to dry overnight in vacuum desiccator.

The surface morphology of the nanocomposites was observed using JEOL SEM-6480LV scanning electron microscope (SEM) operating at 120.0 kV. Samples of Chi/Au and Chi/Au/CNTs were prepared by swelling in distilled water and freeze drying using a Bench-Top Pro Freeze-Dryer. The freeze dried samples were held on a SEM holder by using carbon tape and vacuum dried before coating with gold using an Edwards Sputter Coater-S150B. For energy-dispersive spectrometry (EDX), samples were not coated with gold.

Tensile tests on the films were carried out at room temperature using an Instron model 3369 material tester. A 100 N load cell was used with an extension rate of 2 mm min^{-1}. The samples were cut into dumbbell shape with dimensions 30.3 mm × 0.12 mm × 5.5 mm. Dynamic mechanical thermal analysis (DMTA) was performed on a TRITEC 2000 DMA, Lacerta, using samples cut into strips with dimensions 5.24 mm × 6.73 mm × 0.10 mm. Dynamic mechanical spectra were recorded at a frequency of 1 Hz over a temperature range from 60˚C to 260˚C with a heating rate of 2˚C min^{-1}.

Catalysis Testing

The catalytic efficiency of the nanocomposites was characterized by measuring the rate of reduction of 4-NP to 4-AP. An aqueous solution of 4-NP (20 cm^3, 0.40 mM) was mixed with $NaBH_4$ (50 cm^3, 10 mM). A color change from pale yellow to yellow-green was observed due to the formation of nitrophenolate ions. A 0.1 g piece of nanocomposite membrane was added to the reaction mixture and the progress of the reaction was monitored by tracking changes in the absorption spectra with time.

Results and discussion

Characterization of Au-NPs

The formation of Au-NPs was confirmed by the ruby-red color of the colloidal solution arising from excitation of surface plasmon vibrations. The TEM images of the nanoparticles shown in Fig. 1 (a, b) demonstrate that they are spherical with diameters of 12-15 nm. This is also supported by their UV-Vis spectrum shown in Fig. 1c. The characteristic peak at 520 nm remained unchanged after storage for several weeks in a dark refrigerator.

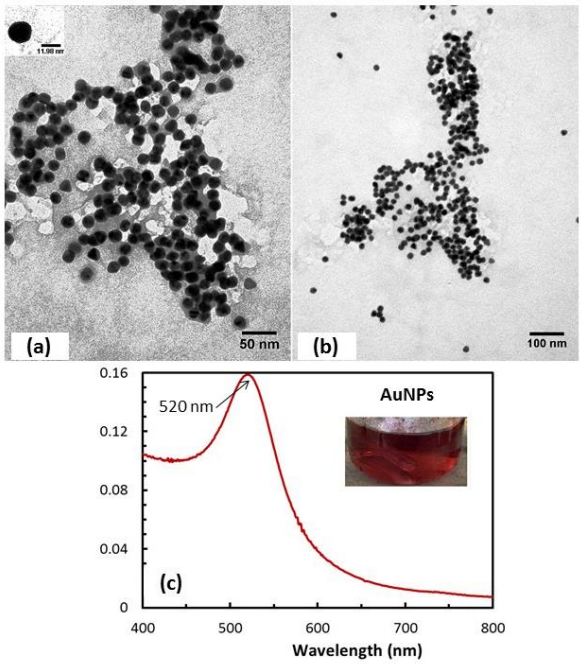

Fig. 1. TEM images (a, b) and UV-Vis spectrum (c) of Au-NPs

Characterization of nanocomposites

Transmission Electron Microscopy. Fig. 2 shows TEM images of nanocomposite films both with (Chi/Au/CNTs, Fig. 2(b)) and without (Chi/Au, Fig. 2(a)) functionalized carbon nanotubes. Both images show uniform distribution of Au-NPs in the polymer matrix. This uniform distribution indicates of the stabilizing ability of chitosan[12, 40] through the large number of hydrophilic groups that can interact with the nanoparticles.[41] It is also notable that the size of the dispersed Au-NPs falls from ~ 12 nm to 9.5 nm. Although this is close to the uncertainty in the measurements, it may be due to the ultrasonication. Okitsu *et al.* reported that the shock waves produced during high intensity sonication can reduce the size of gold nanoparticles.[42] Fig 2b also suggests a homogeneous dispersion of the CNTs in Chi/Au/CNTs nanocomposite.

Scanning Electron Microscopy and infra-red spectroscopy (FTIR). The SEM micrographs and the EDX results for both nanocomposites are shown in Fig. 3. They show that Chi/Au (3A - 3C) exhibited a different morphology than Chi/Au/CNTs (3D - 3G). Elemental analysis by EDX (Fig. 2D and 2H) also confirms the presence of silicon arising from the silane crosslinker. Both nanocomposites are porous although the pore size is larger in Chi/Au than Chi/Au/CNTs. This porous network is responsible for the high degree of swelling reported in the literature.[43] Chi/Au/CNTs has a more compact and thread like surface which can be attributed to more efficient blending of the components in the matrix.[43] The more compact structure of Chi/Au/CNTs also results in increased mechanical strength of the nanocomposite films (see below).

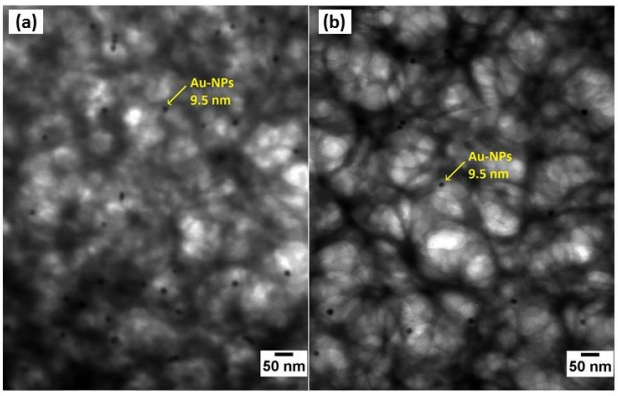

Fig. 2. TEM images of Chi/Au (a) and Chi/Au/CNTs (b) nanocomposites

The FTIR spectra of chitosan and the two nanocomposite membranes are shown in Fig. 4 (a, b). Peaks characteristic of amine and amide groups can be seen around 1650, 1565 and 1370 cm^{-1} in the spectrum of native chitosan. In the spectra of the nanocomposites, these peaks are shifted slightly, suggesting that the complexation of Au-NPs occurs through these groups of chitosan. Peaks characteristic of the CNTs can also be seen around 2100 cm^{-1}. Significantly, there is no change in the spectra after the composite films have been used for catalysis.

Thermo-mechanical Properties. Table 1 illustrates some mechanical properties of the nanocomposite films. The tensile strength and toughness of Chi/Au/CNTs is increased by around a half by the addition of CNTs. The elongation at break is also higher for Chi/Au/CNTs. Further information can be gained from the tensile measurements depicted in Fig 4(c). The increased strength allows a higher stress before breakage and it is interesting that Chi/Au films break since they are brittle whereas Chi/Au/CNTs films show yield behavior. Tang *et al*. also reported that improved strength and toughness arose by incorporating functionalized nanofillers into chitosan[21] while Wang *et al.* also reported that improved mechanical properties of chitosan resulted from the addition of CNTs.[44] The results are also consistent with the SEM images above which show the

uniform distribution of CNTs into the chitosan. This good dispersion suggests high interfacial adhesion via strong polar interactions and hydrogen bonding between the functionalized CNTs and the chitosan matrix which in turn leads to the enhanced mechanical properties.

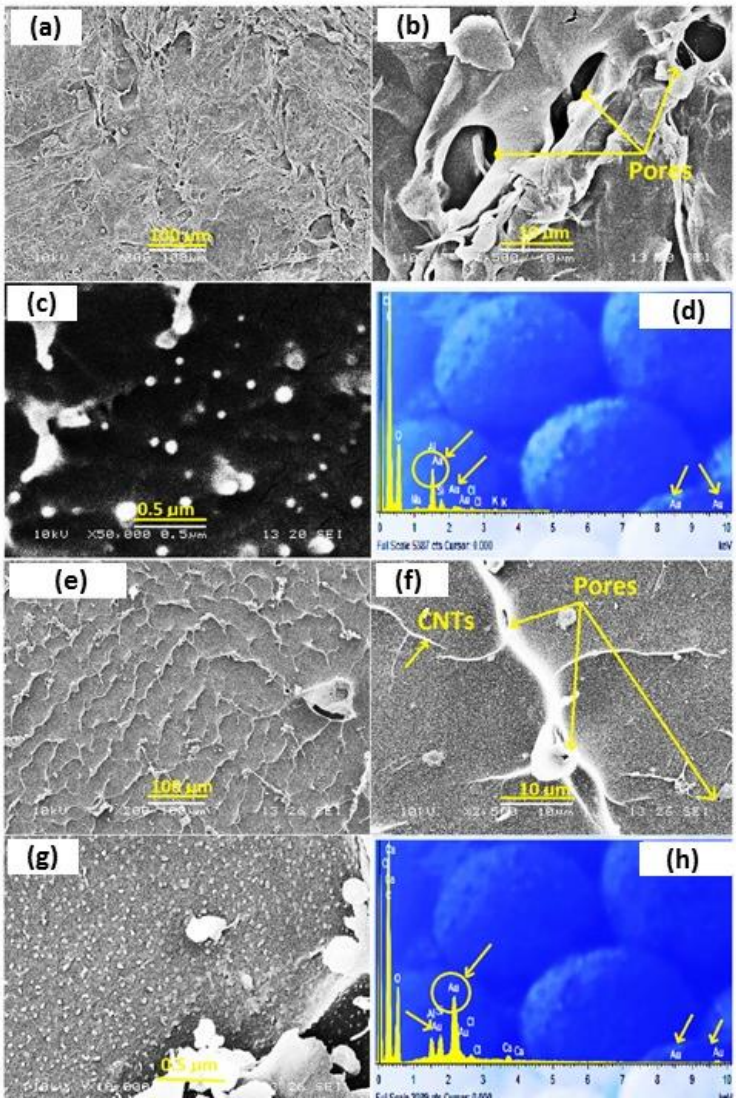

Fig. 3. SEM and EDX images of Chi/Au ((a)-(d)) and Chi/Au/CNTs ((e)-(h)) nanocomposites

Table 1. Mechanical Properties of nanocomposite

Samples	Tensile Strength (MPa)	Elongation at break (%)	Toughness (J m^{-3})
Chi/Au	25.71	3.31	0.40
Chi/Au/CNTs	36.32	4.09	0.70

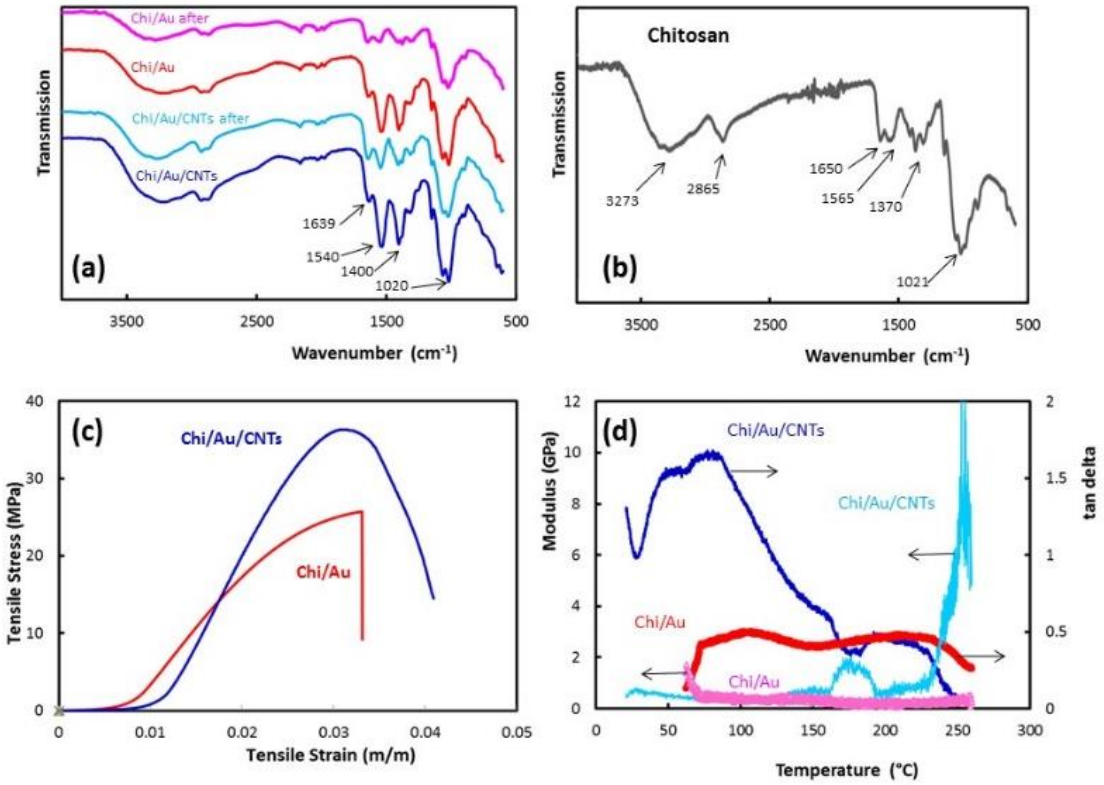

Fig. 4. FT-IR spectra of (a) Gold-Nanocomposites, (b) chitosan. Representative tensile stress-strain curves (c), Storage modulus and tan δ verses temperature for Chi/Au and Chi/Au/CNTs (d).

DMTA is a very useful method for detecting changes of internal molecular mobility and in probing the phase structure and morphology in polymer films and membranes. The DMTA complex spectra of storage modulus (É) and tan δ for Chi/Au and Chi/Au/CNTs are shown in Fig. 4 (d).

There is an indication of transition around 140 °C in Chi/Au although this increases to around 175°C for Chi/Au/CNTs. The storage modulus of Chi/Au/CNTs is much higher at low temperatures indicating a greater ability of the nanocomposites to absorb energy, consistent with the mechanical properties discussed earlier where Chi/Au/CNTs yields under strain while Chi/Au is brittle. The tan δ values are generally similar for both materials at low temperatures. No transitions are observed in Chi/Au but in Chi/Au/CNTs transitions are observed at ~170 °C and at ~250 °C. Such spectra are often associated with glass transitions although it is difficult to see how such transitions could arise in Chi/Au/CNTs and they may be due to changing interactions of the CNTs with the matrix. The storage modulus for Chi/Au/CNTs is significantly higher at low temperatures than the composite without CNTs. This indicates a more elastic solid and is again consistent with the room temperature tensile properties discussed above. This elasticity is lost with temperature and the inclusion of CNTs loses

effect above ~160 °C. However, since catalysis of reactions at or around room temperature is envisaged here, this should have no bearing on our subsequent results.

Catalysis Study

The catalytic activity of the Au-nanocomposite films was tested using the reduction of 4-NP by $NaBH_4$ as a model reaction. The reaction was monitored by UV-Visible spectrometry (Fig. 5). The mixture of 4-NP and $NaBH_4$ shows a λ_{max} at 400 nm, corresponding to the nitrophenolate anion.[48, 49] In the absence of the gold catalyst, this solution is stable and no change in absorbance was observed over several hours. After the addition of a small piece of Chi/Au nanocomposite membrane to the reaction mixture, a gradual decrease in the intensity of the peak at 400 nm was observed (Fig. 5(a)) and the greenish yellow color of the 4-phenolate anion disappeared[50] over a period of around five minutes.[51] The catalysis by Chi/Au/CNTs was also measured under identical conditions with the same mass of gold. The reaction was faster and reduction was complete in less than three minutes. Analysis of the kinetics (Fig. 5(c)) showed that there was a significant induction period before the reduction commenced, presumably due to the time required for the substrate to diffuse into the membrane and encounter the catalytic nanoparticles. This was much reduced in Chi/Au/CNTs indicating that the CNTs make the gold more accessible and facilitating the adsorption of the substrates to react at the catalyst. Once the reaction was established, it proceeded at similar rates in each case, the measured pseudo-first order[52] rate constants being 0.028 s^{-1} for Chi/Au/CNTs and 0.021 s^{-1} for Chi/Au. The probable reaction mechanism is shown in Fig. 6. Significantly, no reaction was observed when pure CNTs, chitosan or chitosan-CNT films were added to the reaction (Fig. 7).

Stability, reusability and recovery of catalyst membrane. For industrial applications, the longer term stability and reusability of a catalyst is very important. As a preliminary exploration, our catalyst films were used a number of times. After each reaction cycle, the nanocomposites were washed three times with distilled water before being introduced to a fresh batch of reactants.

It was found that the Chi/Au catalyst retained its maximum activity for only two cycles. After the third cycle, the high degree of swelling in the reaction mixture and lack of mechanical strength caused the membrane to break up and lose its cohesiveness as shown in Fig. 7. Some reduced catalytic activity was retained since the Au-NPs were still present.

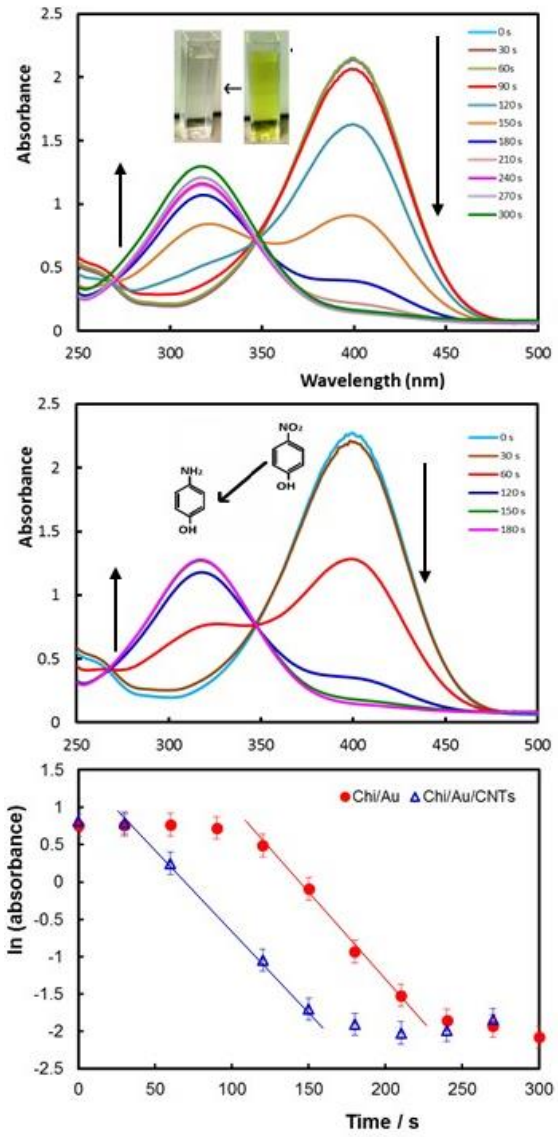

Fig. 5. Borohydride reduction of 4-NP at room temperature. UV-Vis Spectra using Chi/Au (a) and Chi/Au/CNTs (b). First order rate plots (c).

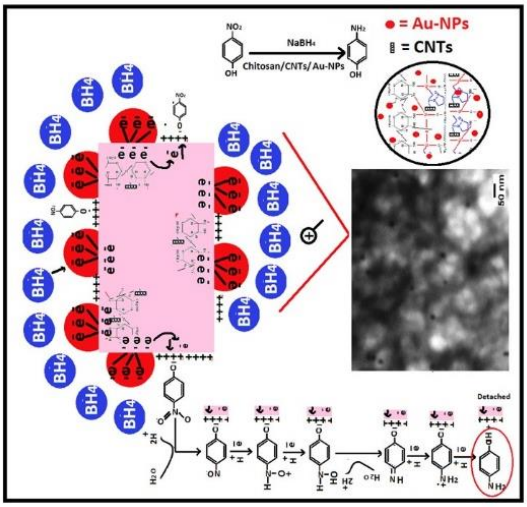

Fig. 6. Probable reaction mechanism of the catalytic activity at the nanocomposite

In contrast the Chi/Au/CNTs membranes remained intact even after 10 recycles and they retained their full catalytic activity. It was also observed that the time to reaction completion did not vary by more than a few seconds. No loss of Au-NPs during the reuse cycle was observed in the absorbance spectra of the product solutions. This is again indicative of the strong interactions between chitosan and the functional groups on the CNTs introduced during irradiation.[39, 45] These interactions not only enhance the mechanical properties of the matrix but also bind the Au-NPs tightly preventing leaching during catalysis.[46, 47]

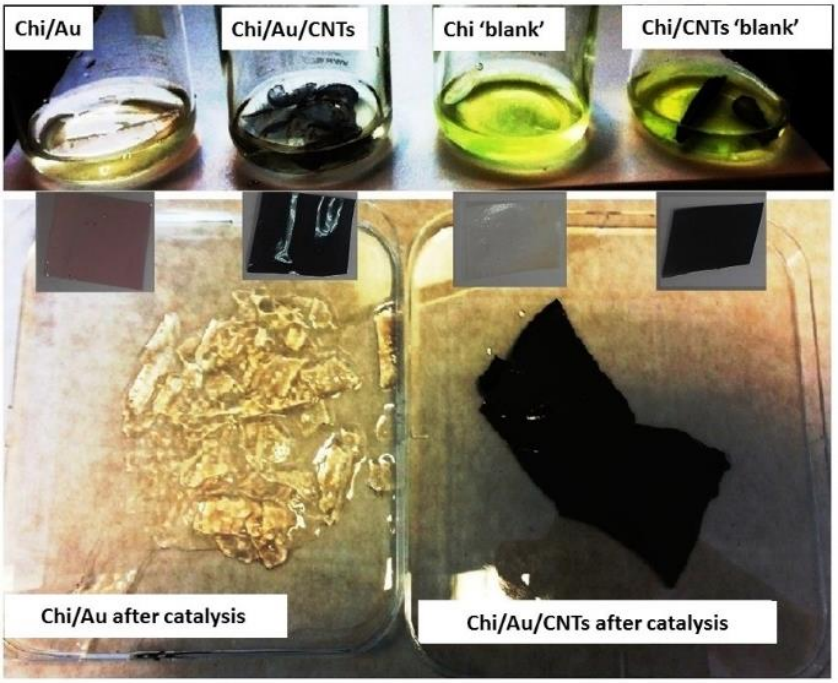

Fig. 7. Photographs of nanocomposite membranes before and after reaction

The recovery of the catalyst after completing the reaction is also an important factor. In many of the published NP catalyzed systems, direct recovery of the NPs is difficult. For example, in the work of Rajesh *et al.,* recovery of the catalyst needs centrifugation.[36] This is one of the primary reasons for employing a support. In our case the catalyst is in the form of a compact membrane which can simply be lifted from the reaction mixture. Although we have not addressed this factor in detail in the present work, there were no signs of loss of Au into the reaction so that recovery should be extremely efficient. Further work is required to completely characterize the long term efficacy and usefulness of our system but the initial results show great promise. The form of the catalyst is also convenient for ready inclusion in a flow system, for example by passing the substrate solution through a filter-bed or by lining a reactor with the nanocomposite membrane. Here, recovery would not be necessary as long as the NPs retain activity for extended periods of time. While further work is needed to characterize the catalytic performance of the membranes using a wider range of more

challenging substrates and a wider range of conditions, the methodology shows considerable promise as a sustainable system for catalyst support.

Conclusions

This work demonstrates the preparation and potential catalytic applications of nanocomposite membranes consisting of gold nanoparticles coated onto CNTs supported in a chitosan matrix. The nanocomposite contained ~ 10 nm diameter gold nanoparticles which were catalytically active for the borohydride reduction of 4-NP. The morphology of the nanocomposite indicated consistent dispersion of the nanoparticles with no agglomeration. The addition of γ-treated CNTs not only accelerated the rate of reaction by significantly shortening the induction time but improved the mechanical strength of the film such that it could be reused up to ten times with no loss of efficiency.

Taking into account the broad prospective of using CNTs as active supports for Au-NPs, the approach outlined here offers new possibilities for the development of various hybrid systems for a diverse range of applications. Most significantly, the synthesized nanocomposites are in the form of membranes which makes them easy to recover and to incorporate into flow systems with a variety of configurations.

Acknowledgements

One of the authors (SB) gratefully acknowledges the Higher Education Commission, Pakistan for providing financial funding under IRSIP to visit the University of Bath. We are grateful to Dr U. Potter and Mr M. Ball for assistance with the electron microscopy and mechanical property measurements respectively.

Notes and references

1 M. H. Mashhadizadeh and R. Pourtaghavi Talemi, *Anal. Meth.*, 2014, **6**, 8956-8964.
2 T. Bhowmik, M. K. Kundu and S. Barman, *RSC Advances*, 2015, **5**, 38760-38773.
3 R. S. Das, B. Singh, S. Mukhopadhyay and R. Banerjee, *Dalton Trans.*, 2012, **41**, 4641-4648.
4 S. Das, A. Pandey, S. Pal, H. Kolya and T. Tripathy, *J. Molec. Liq.*, 2015, **212**, 259-265.
5 K. Sato, K. Hosokawa and M. Maeda, *J. Amer. Chem. Soc.*, 2003, **125**, 8102-8103.
6 G. J. Hutchings, *Catalysis Today* 2005, **100**, 55–61.
7 M. K. Corbierre, N. S. Cameron, M. Sutton, S. G. J. Mochrie, L. B. Lurio, A. Ru¨hm and R. B. Lennox, *J. Amer. Chem. Soc*, 2001, **123**, 10411 -10412.
8 T. Vincent and E. Guibal, *Langmuir*, 2003, **19**, 8475-8483.
9 M. K. Corbierre, N. S. Cameron and R. B. Lennox, *Langmuir*, 2004, **20**, 2867-2873.
10 K. Kuroda, T. Ishida and M. Haruta, *J. Molec. Catal. A,* 2009, **298**, 7-11.

11 D. P. Stankus, S. E, Lohse, J. E. Hutchison and J. A. Nason, *Env. Sci. Technol.*, 2011, **45**, 3238–3244.
12 H. Huang and X. Yang, *Biomacromol.*, 2004, **5**, 2340-2346.
13 H. Huang and X. Yang, *Carbohydrate research*, 2004, **339**, 2627-2631.
14 E. Guibal, *Prog. Polym. Sci.*, 2005, **30**, 71-109.
15 M. N. R. Kumar, *React.Func. Polym.*, 2000, **46**, 1-27.
16 J. J. Hardy, S. Hubert, D. J. Macquarrie and A. J. Wilson, *Green Chem.*, 2004, **6**, 53-56.
17 D. J. Macquarrie and J. J. Hardy, *Ind. Eng. Chem. Res.*, 2005, **44**, 8499-8520.
18 C.-C. Guo, G. Huang, X.-B. Zhang and D.-C. Guo, *Appl. Catal. A*, 2003, **247**, 261-267.
19 M. Zeng, X. Yuan, Z. Yang and C. Qi, *Int. J. Biol. Macromol.*, 2014, **68**, 189-197.
20 A. Islam, M. Riaz and T. Yasin, *Int. J. Biol. Macromol*, 2013, **59**, 119-124.
21 C. Tang, L. Xiang, J. Su, K. Wang, C. Yang, Q. Zhang and Q. Fu, *J. Phys. Chem. B*, 2008, **112**, 3876-3881.
22 C. Tang, N. Chen, Q. Zhang, K. Wang, Q. Fu and X. Zhang, *Polym. Degrad. Stab.*, 2009, **94**, 124-131.
23 D. Aztatzi-Pluma, E. O. Castrejón-González, A. Almendarez-Camarillo, J. F. Alvarado and Y. Duran-Morales, *J. Phys. Chem. C*, 2016, **120,** 2371-2378.
24 P.-C. Ma, S.-Y. Mo, B.-Z. Tang and J.-K. Kim, *Carbon*, 2010, **48**, 1824-1834.
25 F. Banhart, *Rep. Prog. Physics*, 1999, **62**, 1181.
26 T. Saito, K. Matsushige and K. Tanaka, *Physica B: Condensed Matter*, 2002, **323**, 280-283.
27 L. Shi, X. Li, Y. Tuo, H. Jiang, X. Duan and P. Li, *Catal. Today*, 2016.
28 H. Liu, L. Qin, X. Wang, C. Du, D. Sun and X. Meng, *Catal. Commun.*, 2016, **77**, 47-51.
29 K. C. Nguyen, M. P. Ngoc and M. V. Nguyen, *Mater. Lett.*, 2016, **165**, 247-251.
30 W. Feng, L. Zhang, Y. Liu, X. Li, L. Cheng, S. Zhou and H. Bai, *Mater. Sci. Eng. A*, 2015, **637**, 123-129.
31 D. Chen, A. Holmen, Z. Sui and X. Zhou, *Chinese J. Catal.*, 2014, **35**, 824-841.
32 B. Gao, G. Z. Chen and G. Li Puma, *Appl. Catal. B*, 2009, **89**, 503-509.
33 L. Jiang and L. Gao, *Carbon*, 2003, **41**, 2923-2929.
34 Y. Kojima, K.-i. Suzuki, K. Fukumoto, M. Sasaki, T. Yamamoto, Y. Kawai and H. Hayashi, *Int. J. Hydrogen Energy*, 2002, **27**, 1029-1034.
35 J. C. Walter, A. Zurawski, D. Montgomery, M. Thornburg and S. Revankar, *J. Power Sources*, 2008, **179**, 335-339.
36 R. Rajesh, E. Sujanthi, S. S. Kumar and R. Venkatesan, *Phys. Chem. Chem. Phys.*, 2015, **17**, 11329-11340.
37 H. Tsunoyama, H. Sakurai, N. Ichikuni, Y. Negishi and T. Tsukuda, *Langmuir*, 2004, **20**, 11293-11296.
38 J. R. Polte, T. T. Ahner, F. Delissen, S. Sokolov, F. Emmerling, A. F. Thünemann and R. Kraehnert, *J. Amer. Chem. Soc.*, 2010, **132**, 1296-1301.

39 S. Bibi, T. Yasin, S. Hassan, M. Riaz and M. Nawaz, *Mater. Sci. Eng. C*, 2015, **46**, 359-365.

40 A. Primo and F. Quignard, *Chem. Commun.*, 2010, **46**, 5593-5595.

41 A. Murugadoss and H. Sakurai, *J. Molec. Catal. A*, 2011, **341**, 1-6.

42 K. Okitsu, A. Yue, S. Tanabe, H. Matsumoto and Y. Yobiko, *Langmuir*, 2001, **17**, 7717-7720.

43 A. Islam and T. Yasin, *Carbohydrate Polymers*, 2012, **88**, 1055-1060.

44 S.-F. Wang, L. Shen, W.-D. Zhang and Y.-J. Tong, *Biomacromol.*, 2005, **6**, 3067-3072.

45 B. Safibonab, A. Reyhani, A. N. Golikand, S. Mortazavi, S. Mirershadi and M. Ghoranneviss, *Appl. Surf. Sci.*, 2011, **258**, 766-773.

46 Y.-T. Shieh and Y.-F. Yang, *Eur. Polym. J.*, 2006, **42**, 3162-3170.

47 M. Martínez-Morlanes, P. Castell, V. Martínez-Nogués, M. T. Martinez, P. J. Alonso and J. Puértolas, *Composites Sci. Technol.*, 2011, **71**, 282-288.

48 A. G. Majouga, E. K. Beloglazkina, E. A. Manzheliy, D. A. Denisov, E. G. Evtushenko, K. I. Maslakov, E. V. Golubina and N. V. Zyk, *Appl. Surf. Sci.*, 2015, **325**, 73-78.

49 K. Esumi, R. Isono and T. Yoshimura, *Langmuir*, 2004, **20**, 237-243.

50 H. Wu, X. Huang, M. Gao, X. Liao and B. Shi, *Green Chem.*, 2011, **13**, 651-658.

51 S. Wunder, F. Polzer, Y. Lu, Y. Mei and M. Ballauff, *J. Phys. Chem. C*, 2010, **114**, 8814-8820.

52 C. Lin, K. Tao, D. Hua, Z. Ma and S. Zhou, *Molecules*, 2013, **18**, 12609-12620.